Appl. Phys. A 00, 1–6 (2003)
DOI: 10.1007/s00339-003-2220-7

Applied Physics A
Materials Science & Processing

K.M. SMITH[1,✉,*]
M.Y. HUSSAINI[1,*]
L.D. GELB[2,**]
S.D. ALLEN[3,***]

Modeling laser-assisted particle removal using molecular dynamics

[1] School of Computational Science and Information Technology, Florida State University Tallahassee, FL 32306-4120
[2] Department of Chemistry Washington University St. Louis, MO 63130
[3] Department of Chemistry and Biochemistry Florida State University Tallahassee, FL 32306

Received: 24 January 2003/Revised version: 10 May 2003
Published online: ■ ■ 2003 • © Springer-Verlag 2003

ABSTRACT Laser-assisted particle removal, a method of cleaning nano- to micro-scale particles from surfaces, was modeled using molecular dynamics. A two-dimensional molecular model consisting of substrate, particle, and adsorbed fluid was used. In order to obtain statistical accuracy of cleaning efficiencies, over 1200 particle-removal simulations were conducted. The effects of fluid thickness and substrate temperature were both considered, and good qualitative agreement with experimental results was obtained. The molecular dynamics approach is shown to be an effective way to study these systems.

PACS 81.65.Cf; 79.20.Ds

1 Introduction

Laser-assisted particle-removal techniques include both dry laser cleaning and 'steam laser cleaning' [1]. As the names imply, dry laser cleaning is performed without liquid present, while steam laser cleaning is performed with the addition of a liquid film. However, since liquid is present in both cases unless dry laser cleaning is carried out in a strong vacuum, we prefer to call cleaning with a deposited liquid 'energy-transfer cleaning', since the added liquid film acts as an energy-transfer medium.

Energy-transfer cleaning (ETC) is a technique for removing small particles (as small as 50 nm, though currently used principally for particles of ~ 1 μm diameter) from a substrate. In this process, a small amount of energy-transfer medium (ETM) is condensed onto the substrate and then laser energy is directed at the substrate surface. This energy is absorbed by the ETM, and perhaps also by the substrate and/or the particle, and results in removal of the ETM and the particle. A single optimized laser pulse has been shown to effectively remove 90% of particles with sizes on the order of 1 μm [2]. Repeating the process allows a removal efficiency of near 100% to be achieved, typically within five to eight repetitions [2].

Particle removal is thought be caused by a combination of three mechanisms: explosive boiling of the ETM, thermal expansion of the particle ('hopping' effect), and thermal expansion of the substrate ('trampoline' effect) [1]. Additionally, the local ablation of the substrate beneath the particle is a mechanism for particle removal, although one we wish to avoid since particle removal without substrate damage is desired. Previous treatments of ETC have estimated the main contributions (van der Waals attractions and capillary forces) to particle adhesion, and compared the total adhesive force to a model of the removal force, where the removal force due to explosive boiling arises from the stress wave produced at the vapor/liquid interface [3, 4]. In addition, forces due to the thermal expansion of the particle and surface can be estimated. While appropriate for macroscopic particles and thick fluid layers, such theories are not necessarily applicable to nano-scale systems, and lack the ability to treat irregular particles, rough surfaces, and very thin ETM films.

There have been three-dimensional molecular dynamics models of explosive boiling of thin liquid films on a substrate [5, 6]. For these simulations, the liquid layers are composed of 6, 12, 24, 36, or 48 layers of water molecules layered on a gold substrate that is heated to 1000 K. These studies have focused on 'matrix-assisted laser-induced desorption' (MALDI) processes in which explosive heating of a solid ETM is used to project relatively large molecules into the vapor phase for further analysis. The ETC system considered here has not, to our knowledge, been previously treated with molecular-scale simulations.

2 Simulation model

The goal of this study is to obtain good statistical accuracy of cleaning efficiencies, which requires performing particle-removal simulations many times. With the idea of conducting a very large number of simulations, a simple two-dimensional molecular model was constructed for the particle-removal system, consisting of a substrate, ETM fluid, and particle. The reduced dimensionality of the system greatly decreases the number of molecules that must be simulated in order to access the desired length scales, lowering the computational cost of the study. To further reduce computational

✉ Fax: +1-850/644-0098, E-mail: ksmith@csit.fsu.edu
*Fax: +1-850/644-0098, E-mail: myh@csit.fsu.edu
**Fax: +1-314/935-4481, E-mail: gelb@wuchem.wustl.edu
***Present address: Arkansas State University, PO Box 179, State University, AR 72467, USA
Fax: +1-870/972-2036, E-mail: sdallen@astate.eduS

requirements, a very simple molecular model was applied. All interactions between molecules in the ETM, substrate, and particle were modeled using the Lennard–Jones 12-6 potential [7]:

$$\varphi(r_{ij}) = 4\varepsilon\left[\left(\frac{\sigma}{r_{ij}}\right)^{12} - \left(\frac{\sigma}{r_{ij}}\right)^{6}\right], \quad (1)$$

where r_{ij} is the distance between molecules i and j, σ is a measure of the molecule's diameter (the distance where the energy is zero), and $-\varepsilon$ is the minimum value of the energy. The simulations were run using reduced units [7], with the mass of all particles equal. (Appendix A describes the conversion from reduced units to dimensional units for argon molecules. For clarity, we will present both reduced and dimensional values.) The Lennard–Jones potential parameters for the interactions between the ETM, particle, and substrate are given in Table 1. The potential interactions between all molecules were truncated at 2.5σ (0.85 nm), for additional time savings.

The values in Table 1 were chosen according to the following rationale. The fluid parameters are set equal to 1.0, making it the reference material. The value of 1.5, chosen for both the fluid–substrate ε and the fluid–particle ε, is high enough to ensure that the fluid wets both solids at all the temperatures considered in this study. The high value (10.0) for the particle–particle ε was chosen to ensure that the particle remains solid at the elevated temperatures reached in the removal simulations.

The substrate is composed of five layers of molecules arranged in a hexagonal lattice, which is the two-dimensional crystal structure of the Lennard–Jones solid. During the simulation, the molecules of the substrate interact with nearby fluid and particle molecules, but the substrate molecules are held in fixed positions. This is partly for additional computational cost savings, but mainly because thermal expansion of the substrate in the periodic geometry would likely cause buckling, which would substantially complicate our analysis. The rigid-substrate approximation avoids this, although it does mean that the 'trampoline' mechanism for particle removal is not present in these simulations.

The particle is circular, with a diameter of 19σ (6.46 nm), and is also composed of molecules in a hexagonal arrangement. The lowest layer of molecules that compose the particle are in contact with the molecules in the uppermost layer of the substrate.

Simulations were conducted on a two-dimensional computational domain of size $x = 202\sigma$ (68.68 nm) by $y = 240\sigma$ (81.6 nm). The domain is periodic in x and molecules that reach the maximum y value are reflected back into the domain. If a 'free' upper boundary were used, the liquid would, at equilibrium, have entirely boiled away into the vacuum with none remaining on the surface; this is trivially predicted by the zero-pressure limit of the Langmuir isotherm. Therefore, in order to maintain the liquid layer, the total system volume must be constrained by an upper boundary. Since the important part of the simulation occurs in the lower part of the domain, the reflection condition has no effect on the results that follow.

After placing a particle on the substrate within a computational cell, fluid is added to the cell by performing a grand canonical Monte Carlo (GCMC) simulation. GCMC is a stochastic technique in which the number of particles is allowed to vary according to a specified chemical potential [7]. This is accomplished through 'moves' in which molecules are either displaced, created at random positions, or destroyed. The values of the chemical potential, the average thickness of the resulting layer, and the number of molecules in the domain are presented in Table 2. When completed, as determined by stabilization of the total number of particles, a liquid (ETM) film of varying thickness overlies the substrate and the particle, as shown in Fig. 1.

Because particle removal is a discrete event, in order to determine removal efficiency it is necessary to simulate the removal process many times, starting from various initial con-

Interaction	σ	ε
ETM–ETM	1.0	1.0
ETM–particle	1.0	1.5
Particle–particle	1.0	10.0
ETM–substrate	1.0	1.5
Particle–substrate	1.0	1.5

TABLE 1 Lennard–Jones potential parameters for interactions between the ETM, particle, and substrate

Chemical potential	Film thickness	Number of fluid molecules
−1.67	3σ	1756
−1.66	6σ	2149
−1.6495	10σ	2927
−1.649	25σ	5093
−1.648	50σ	7755
−1.646	70σ	10992

TABLE 2 Chemical potential values used in grand canonical Monte Carlo simulation, the thickness of the resulting layer, and the number of particles in the domain

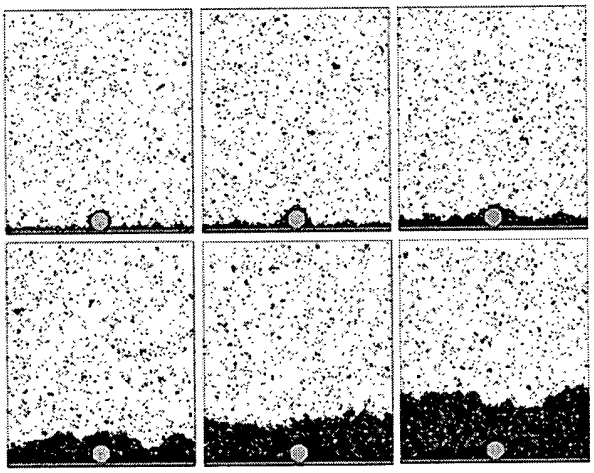

FIGURE 1 Initial configurations for the fluid thicknesses 3σ (1.02 nm), 6σ (2.04 nm), 10σ (3.4 nm), 25σ (8.5 nm), 50σ (17 nm), and 70σ (23.8 nm), respectively. The substrate is *dark gray*, the particle is *light gray*, and the fluid molecules are *black*. Particle diameter is 19σ (6.46 nm)

ditions. For each configuration shown in Fig. 1, an additional nine configurations were generated by allowing the GCMC simulation to run for an additional short time (100 cycles). Thus, 10 equilibrated configurations were available for each fluid thickness considered.

In the molecular dynamics simulations, a fifth-order Gear predictor–corrector algorithm was used to integrate the equations of motion, with a time step of 0.005 reduced units (1.1×10^{-14} s). After 250 time steps, the substrate temperature was instantaneously increased from its base value of 0.4 (48.4 K) to a value between 0.5 (60.5 K) and 5.0 (605 K). For comparison, the critical temperature of the two-dimensional Lennard–Jones fluid is approximately 0.5 [8]. Increasing the substrate temperature in this manner approximates the effect of laser heating in the case that the laser energy is absorbed by the substrate, rather than the fluid; the possibility of energy transfer directly into the fluid was not considered in this study. In the simulation, the substrate temperature is enforced by applying a 'Gaussian isokinetic'-type thermostat to fluid molecules which are within a distance of 2.5σ (0.85 nm) of the substrate. That is, the fluid layer in immediate contact with the substrate is given a fixed temperature equal to the substrate temperature, accomplished by constraining the total kinetic energy of the fluid particles in that region.

Each simulation was run for 30 000 time steps (0.33 ns), which, except in the case of temperature equal to 0.5 (60.5 K), was enough to observe the complete ejection of the ETM layer, and perhaps particle removal.

3 Results

In simulations where no ETM was present, i.e. no fluid film was present, particle removal was not observed at any temperature between 0.5 (60.5 K) and 5.0 (605 K).

When ETM was present, particle removal was observed for various temperatures and ETM film thicknesses. Particle removal was defined as the particle lifting with the fluid and remaining well above the substrate surface at the end of the simulation. It was possible for the particle to lift slightly with the removal of the fluid film, but then to fall back onto the substrate. Recall that, for each film thickness, 10 simulations were conducted, each with a slightly different initial condition.

These simulations show that when the substrate is heated to a temperature of 0.5 (60.5 K), the liquid layer slowly (on a molecular time scale) evaporates, and no particle removal is observed, i.e. the particle is still in contact with the substrate after the final time step. For substrates heated to temperatures between 1.0 (121 K) and 1.1 (133.1 K), the ETM explosively leaves the surface, but no particle removal was observed. At temperatures above 1.2 (145.2 K), particle removal was observed, although not all simulations for a given ETM film thickness at a given temperature lead to particle removal. As an example, snapshots from two simulations of the 10σ (3.4 nm) film thickness at a substrate temperature of 1.6 (193.6 K) are shown in Fig. 2. In the simulation depicted in the upper row of Fig. 2, particle removal is observed, but in the second simulation, depicted in the lower row, particle removal is not observed. In both simulations, the departing fluid layer coalesces into droplets at late times (far right). Droplet formation has been observed in experimental studies of particle removal [9].

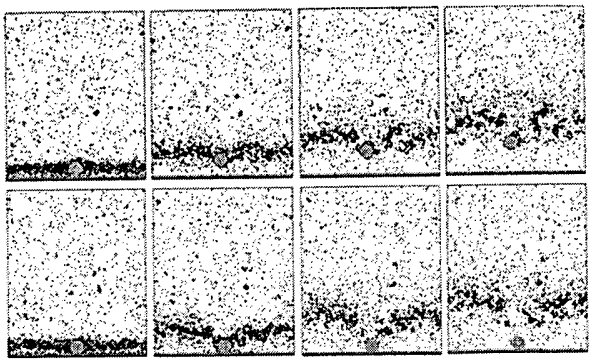

FIGURE 2 Snapshots of two simulations of the 10σ (3.4 nm) film thickness with a substrate temperature of 1.6 (193.6°K). From *left* to *right*, the elapsed time is 20 (2.2×10^{-13} s), 40 (4.4×10^{-13} s), 60 (6.6×10^{-13} s), and 80 (8.8×10^{-13} s) reduced time units, respectively. The *upper row* shows a simulation where there is particle removal, while the *lower row* shows a simulation, at the same temperature, where particle removal does not occur

Particle removal is summarized in Table 3, which presents the cleaning efficiency (percentage of particles that are removed from the substrate) as a function of ETM film thickness and surface temperature. Note that simulations were conducted for at least 14 different substrate temperatures for each fluid-film thickness.

The high end of the temperature range (> 3.0 or > 363 K) is sufficient to melt the particle with or without the presence of ETM. For the 70σ (23.8 nm) thick film, at temperatures of 3.0 (363 K) and 3.5 (423.5 K), there was one simulation (out of 10) where the ETM was removed, but the particle was not removed, as shown by the 90% removal efficiencies in Table 3. In both of these cases, the particle deformed, as shown in Fig. 3.

Temp	3σ	6σ	10σ	25σ	50σ	70σ
1.0	0%	0%	0%	0%	0%	0%
1.1			0%			
1.2			30%	0%	0%	
1.3			50%	0%	30%	
1.4		0%	50%	20%	50%	
1.5	0%	20%	50%	20%	40%	0%
1.6	0%	60%	90%	90%	60%	10%
1.7	0%	30%	70%	100%	50%	20%
1.8	0%	50%	100%	80%	80%	40%
1.9	10%	30%	100%	90%	100%	50%
2.0	10%	90%	90%	100%	80%	50%
2.5	60%	90%	100%	100%	100%	100%
3.0	80%	90%	100%	100%	100%	90%
3.5	100%	100%	100%	100%	100%	90%
4.0	100%	100%	100%	100%	100%	100%
4.5	100%	100%	100%	100%	100%	100%
5.0	100%	100%	100%	100%	100%	100%

TABLE 3 Cleaning efficiency (as percentage of particles removed from the substrate) for all fluid layers. No entry means a simulation was not conducted at that temperature, but the cleaning efficiency can be assumed to be 0% at that temperature, since simulations run at both higher and lower temperatures gave cleaning efficiencies of 0%

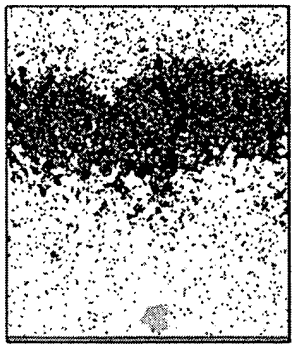

FIGURE 3 70σ (23.8 nm) thick fluid layer heated to a temperature of 3.0 (363°K) at the final time (0.33 ns), illustrating the deformation of the particle. The substrate is *dark gray*, the deformed particle is *light gray*, and the fluid molecules are *black*

For additional analysis, the net fluid and particle velocities were averaged over the 10 simulations for each film thickness and temperature, and the maximum velocities of the departing fluid and particle were determined. These maximum velocities as a function of substrate temperature are shown in Fig. 4. The fluid velocities increase with increasing temperature, and are all reasonably comparable, with the thinnest and thickest ETM layers exhibiting the lowest velocities at high temperatures. The cleaning threshold, defined to be the intersection of the particle-velocity curve with the temperature axis, increases with both increasing and decreasing fluid-film thickness. Particle velocities (at surface temperatures above the cleaning threshold) are more sensitive to fluid-film thickness than are fluid velocities. The fluid and particle velocities for the 10σ (3.4 nm), 25σ (8.5 nm), and 50σ (17 nm) film thicknesses are similar. It appears that each of these film thicknesses is thick enough for efficient transmission of substrate energy and yet not so thick as to impede the upward motion of the energized layer. For very thin films (3σ (1.02 nm) and 6σ (2.04 nm)), there are fewer fluid molecules near the particle, and higher substrate temperatures are required to transmit sufficient energy to the ETM film for particle removal, so particle velocities are reduced and the cleaning threshold temperatures are higher. For very thick films (70σ or 23.8 nm), the inertia of the overlaying fluid layer causes the particle velocity to be reduced and, again, particle velocities are reduced and the cleaning threshold occurs at higher temperatures.

To investigate the effects of ETM fluid viscosity on particle-removal efficiency, additional simulations were conducted using a fluid with a molecular mass of 2.0 (instead of 1.0) for the 10σ (3.4 nm) and 50σ (17 nm) thick films. (By increasing the mass, we are changing the time scale, and thus the time autocorrelation function of the pressure [7], resulting in an increased bulk viscosity.) As before, 10 simulations were conducted for each fluid thickness, the net fluid and particle velocities were averaged, and the maximum velocity of the fluid and particle was determined. The resulting data for the maximum velocities of the fluid and particle as functions of substrate temperature are shown in Figs. 6 and 5. For both films, at each temperature the more viscous (massive) fluid has a lower departure velocity than the original fluid. For the 10σ (3.4 nm) film (Fig. 6), the particle velocities are approximately equivalent, but for the 50σ (17 nm) film (Fig. 5), the particle velocities in the high-viscosity fluid are reduced at high temperatures. This is likely due to the inertial effect described above, i.e. the fluid mass above the particle hinders its removal. Such an effect might be enhanced at high temperatures, when higher removal velocities are expected.

Experimental ETC results are usually presented as functions of laser fluence, rather than surface temperature, as that is the experimental control variable. In order to make more meaningful comparisons between our simulations and experiments, we determined the total energy input into the complete (fluid+particle) system. The total energy consists of a potential contribution (principally the cohesive energy of the fluid and the adsorption energy of the fluid to the substrate and particle) and a kinetic contribution. The total energy is observed to rise steeply (due to the addition of kinetic energy, which simulates the heat transferred to the fluid from the hot substrate) until there is no longer any fluid in contact with

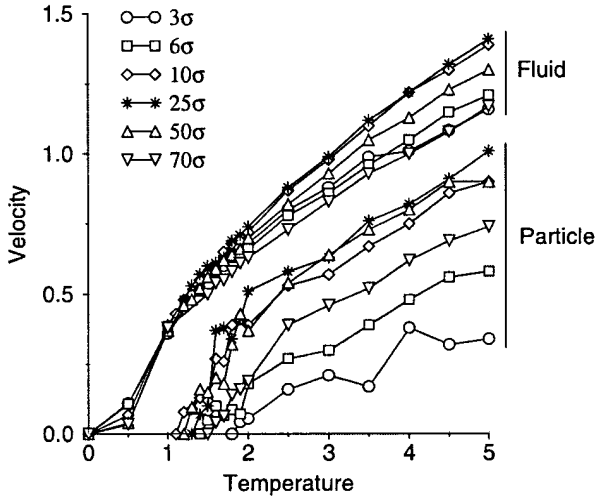

FIGURE 4 Maximum velocity as a function of substrate temperature for the fluid and the particle as the thickness of the fluid layer varies

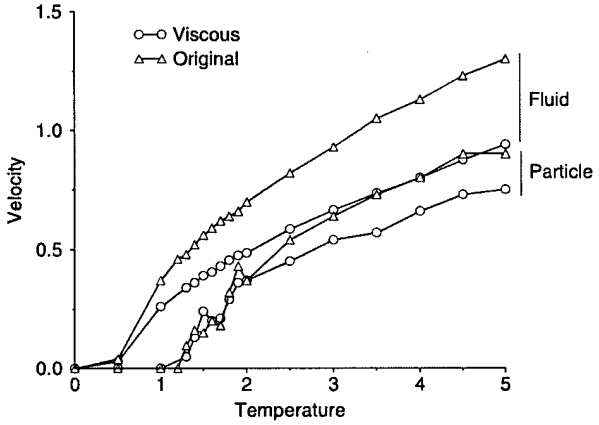

FIGURE 5 Fluid and particle maximum velocity as functions of substrate temperature for the original fluid and for a fluid with twice the viscosity of the original for the 10σ (3.4 nm) thick film

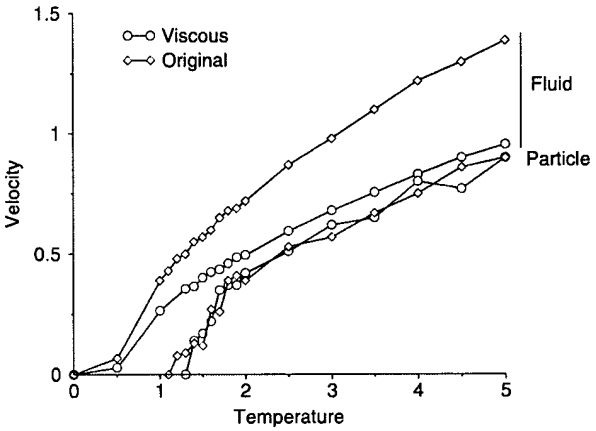

FIGURE 6 Fluid and particle maximum velocity as functions of substrate temperature for the original fluid and for a fluid with twice the viscosity of the original for the 50σ (17 nm) thick film

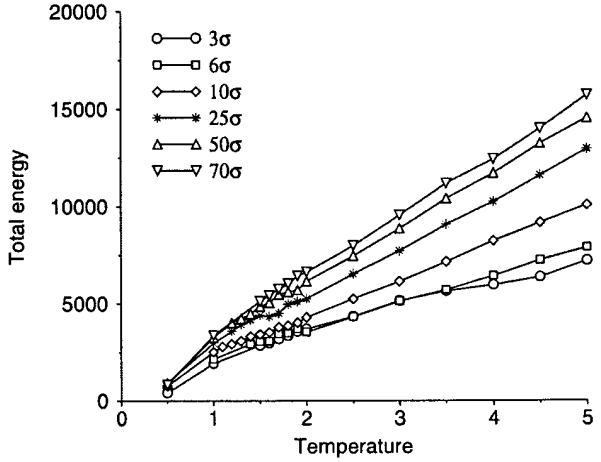

FIGURE 8 Total energy plotted as a function of surface temperature for varying fluid-film thicknesses

the surface, after which efficient energy transfer is no longer possible, and the energy input levels off very quickly. In an experimental system, if the laser pulse time is short in comparison with the elapsed time to particle removal, it is reasonable to say that the laser fluence is a measure of the total energy input into the complete system, because the fluid and particle remain on the surface during the entire pulse. For particles that are removed during the laser pulse, this is not the case. Mosbacher et al. [10] used pulse times (FWHM) of 2.5 ns and 7 ns, which are very short in comparison with experimental removal times. They found a single fluence threshold for ETC of particles that are 60, 500, and 800 nm in diameter with films that are 200–400 nm thick that is also independent of particle composition. The ratios of film thickness to particle diameter used in these experiments are similar to those used here (0.16–3.7). Figure 7 shows the cleaning efficiency (given as percentage of particles removed) as a function of total energy input into the system. As in the experimental results, we observe a nearly universal cleaning threshold (steep rise) in all data sets except the thickest one. Again, as particle removal

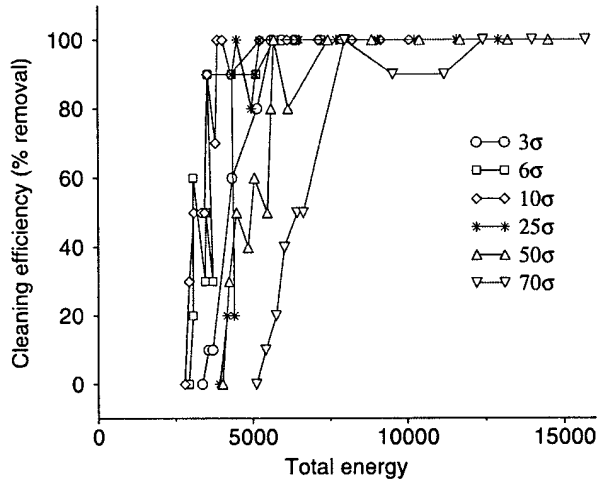

FIGURE 7 Cleaning efficiency (given as percentage of particles removed) as a function of total energy input into the system

appears to be hindered by very thick films, as explained above, it is consistent that the most energy must be transferred into the thick-film system in order to overcome inertial resistance.

Figure 8 shows the total energy transferred to the complete (fluid+particle) system as a function of substrate temperature. This figure shows that, for most of the systems studied, the energy transferred is a linear function of the surface temperature for temperatures above the removal threshold. While the rate of energy transfer should certainly be linear with the temperature difference of the surface and fluid, the time that the fluid and particle remain on the surface is a complicated function of the fluid thickness and the surface temperature, so it is somewhat surprising that the total energy transferred is also linear. At low temperatures, near and below the removal threshold, the linearity is broken, because the mechanism of energy transfer changes; explosive boiling does not occur at low temperatures, and the particle is not always removed.

We note that the periodic boundaries used in this simulation are a potential source of unphysical behavior due to the suppression of long-wavelength density fluctuations in the fluid. That is to say, a very narrow periodic cell may act to stabilize a liquid 'slab' of fluid by suppressing density fluctuations, rather than allowing the fluid to break up into droplets. However, in evaluating the approximations made in this study, a series of preliminary simulations were run using a smaller computational domain measuring $x = 67\sigma$ (22.78 nm) by $y = 120\sigma$ (40.8 nm), with very similar results. The invariance with box size suggests that the long-wavelength fluctuations are not being suppressed in these simulations.

4 Summary

Energy-transfer cleaning of nano-sized particles was simulated using molecular dynamics and a simple two-dimensional model based on the Lennard–Jones potential. The simplicity of the model allowed for a comprehensive study of the effects of heating intensity (through surface temperature) and fluid-film thickness. Although the particle

modeled here is two to three orders of magnitude smaller than those studied experimentally so far, the behavior observed in the model is in good qualitative agreement with experimental results. This indicates that further studies using more realistic molecular models and three-dimensional systems would aid in developing a complete microscopic picture of the phenomena involved in ETC and similar processes. Points of positive qualitative agreement with experiments are:

- The simulated system clearly exhibits sharp ETC thresholds, which are largely independent of the fluid-film thickness [10].
- Thicker fluid layers lead to lower particle-ejection velocities at a given temperature (fluence) [11].
- Cleaning efficiencies above the threshold are close to 90% [2, 12].
- The simulated fluid undergoes immediate explosive vaporization from the surface layer, which is presumed to occur in the experimental systems [13, 14], and is incorporated into standard one-dimensional models of ETC [15].
- Aerosol formation is observed in the ejected fluid layer [9].
- The ratio of fluid-layer thickness to particle diameter does not substantially affect the removal threshold or efficiency [10].
- Changes in liquid properties do substantially affect these quantities [16, 17].

A substantial finding from this study is that even fluid layers as thin as one or two molecules can contribute substantially to particle removal. Many experimental surfaces (except for those prepared in ultra-high vacuum) will have at least this quantity of adsorbed gases present at ambient or low-vacuum conditions. Thus, experimental studies of 'dry laser cleaning', in which only hopping and trampolining effects are expected to contribute to particle removal, may well also contain an element of ETC due to such adsorbed layers. This work indicates that, for small particles, this contribution can be substantial.

Quantitative modeling of this system would require fully three-dimensional simulations and more realistic potential models for the fluid and solids. Most experimental work is done on particles of 60 nm diameter and larger, and accessing such length scales would involve simulating millions of atoms, instead of thousands, greatly increasing the computational cost. Another important approximation that could be added in a more sophisticated model would be to directly model the laser fluence and the dynamics of the solid substrate, which would both re-introduce trampolining effects, and would allow modeling of different laser pulse shapes, as used in experiments.

5 Reduced Units

When simulating only one type of molecule, the mass of the molecule serves as a fundamental unit. The Lennard–Jones potential is completely determined by the parameters σ and ε. If $\sigma = \varepsilon = 1$, then calculations can be made in reduced units [7], and other properties (e.g. density, temperature, energy, time, etc.) can be written in terms of σ, ε, and mass.

The results presented here are in reduced units. However, they can be easily converted to specific units by choosing appropriate values of σ, ε, and mass. For argon, $\sigma = 0.34$ nm, $\varepsilon = 1.67 \times 10^{-21}$ J, and the mass is 6.69×10^{-26} kg. Using these values, the diameter of the particle is 6.5 nm, the thickness of the fluid film varies from 1.0 nm to 23.8 nm, and the size of the computational domain is $x = 68.7$ nm by $y = 81.6$ nm. One time step of 0.005 is equivalent to 1.1×10^{-14} s, and each simulation was run for 0.33 ns. One reduced unit of temperature is equivalent to 121 K, one reduced unit of velocity is equal to 154.5 m/s, and one reduced unit of energy is equal to 1.67×10^{-21} J/mol.

REFERENCES

1 A.C. Tam, W.P. Leung, W. Zapka, W. Ziemlich: J. Appl. Phys. **71**, 3515 (1992)
2 S.D. Allen, A.S. Miller, S.J. Lee: Mater. Sci. Eng. B **49**, 85 (1997)
3 Y.-F. Lu, Y. Zhang, W.-D. Song, D.S.H. Chan: Jpn. J. Appl. Phys. **37**, L1330 (1998)
4 Y.F. Lu, W.D. Song, M.H. Hong, Y.W. Zheng, T.C. Chong: Tribol. Int. **33**, 329 (2000)
5 Y. Dou, L.V. Zhigilei, Z. Postawa, N. Winograd, B.J. Garrison: Nucl. Instrum. Methods B **180**, 105 (2001)
6 Y. Dou, L.V. Zhigilei, N. Winograd, B.J. Garrison: J. Phys. Chem. A **105**, 2748 (2001)
7 M.P. Allen, D.J. Tildesley: *Computer Simulation of Liquids* (Oxford University Press, New York 2001)
8 R.R. Singh, K.S. Pitzer, J.J. de Pablo, J.M. Prausnitz: J. Chem. Phys. **92**, 5463 (1990)
9 S.J. Lee, K. Imen, S.D. Allen: J. Appl. Phys. **74**, 7044 (1993)
10 M. Mosbacher, V. Dobler, J. Boneberg, P. Leiderer: Appl. Phys. A **70**, 669 (2000)
11 S.I. Kudryashov, S.D. Allen: Appl. Phys. Lett. (in press) CE?
12 M. Mosbacher, N. Chaoui, J. Siegel, V. Dobler, J. Solis, J. Boneburg, C.N. Afonso, P. Leiderer: Appl. Phys. A **69** [Suppl.], S331 (1999)
13 H.K. Park, D. Kim, C.P. Grigoropoulos, A.C. Tam: J. Appl. Phys. **80**, 4072 (1996)
14 O. Yavas, A. Schilling, J. Bischof, J. Boneberg, P. Leiderer: Appl. Phys. A **64**, 331 (1997)
15 X. Wu, E. Sacher, M. Meunier: J. Appl. Phys. **87**, 3618 (2000)
16 Y.P. Lee, Y.F. Lu, D.S.H. Chan, T.S. Low, M.S. Zhou: Jpn. J. Appl. Phys. **37**, 2524 (1998)
17 Y.F. Lu, Y. Zhang, Y.H. Wan, W.D. Song: Appl. Surf. Sci. **138–139**, 140 (1999)

CE? Please update this reference.

Editor's or typesetter's annotations (will be removed before the final TEX run)